



## Measurement of infrared radiation emitted by the flame of a vegetation fire

G. Parent, Z. Acem, S. Lechêne, P. Boulet\*

LEMTA, Nancy-Université, CNRS, Faculté des Sciences et Techniques, BP 70239, 54506 Vandœuvre lès Nancy Cedex, France

### ARTICLE INFO

#### Article history:

Received 19 February 2009

Received in revised form

24 August 2009

Accepted 24 August 2009

Available online 19 September 2009

#### Keywords:

Emission

Infrared radiation

Flame

Fire

### ABSTRACT

An experimental study has been carried out on the radiation emitted in the infrared by a flame produced by the combustion of vegetation (vine branches) in a square tray of size 50 × 50 cm. Measurements have been performed with an FTIR spectrometer and an IR camera on the corresponding flame with characteristic height between 50 cm and 1 m. A specific device has been built in order to allow the simultaneous acquisition of spectra in the range between [1000–6000 cm<sup>-1</sup>] and pictures in selected bands of the infrared. Pictures with a camera in the visible range have been taken at the same time. A preliminary calibration using a reference emitter has been done in order to evaluate the emitted radiation quantitatively. By comparing the emission by flames with the one of this reference surface, the radiation emitted by a vegetation flame has been observed and analysed as a function of the wavenumber. The emission is observed to be predominant in a range around 2300 cm<sup>-1</sup>, due to CO<sub>2</sub> production, and strong emission bands related to H<sub>2</sub>O are also observed. The experimental tools, FTIR spectrometer and IR camera, both in good agreement, show a weak emission due to soots, at least at this scale of relatively small flames.

© 2009 Elsevier Masson SAS. All rights reserved.

### 1. Introduction

Radiative transfer is well known to play a key role in the propagation of fires, as stated for example in some of the review articles devoted to fire sciences and to radiation [1–3]. Taking it into account in a satisfactory way is a hard task, however. Two types of difficulties can be especially mentioned in relation with this heat transfer mode: (i) the modelisation itself is not straightforward yielding a well known but complex basic equation, the Radiative Transfer Equation (RTE) for which approximate solutions are often far from being accurate, whereas numerical solutions require high computational means; (ii) the radiative properties used as input data in these equations must be known with sufficient accuracy. These latter properties characterize the emitted radiation (to be described as a function of direction, space location, time and wavelength) and the radiative properties of the lighted surfaces: all surfaces illuminated by the flames and especially the vegetation in the frame of forest fires, the underlying focus of the present study. The present authors are involved in a characterization task devoted to the radiative properties in the frame of a project supported by the French National Research Agency (ANR), on the protection against forest fires. Following recent contributions to fire propagation modeling whatever the complexity of the model itself, or

more generally studies focused on vegetation fires, the need for radiative properties is still crucial. It appears for example in [4–8] among others, where all topics related to radiation are addressed: from modeling purpose, to flux measurement, and to vegetation or flame property identifications. We have recently addressed the problem of characterizing the vegetation properties in terms of transmission, reflection and absorption [9]. An experimental study has been carried out in the infrared range, approximately from 1000 to 6000 cm<sup>-1</sup> (or from 1.6 to 10 μm). Considering an irradiation by a source at a temperature around 1000 K, and following the Wien's law, the maximum of radiation emission would be at 2.9 μm and the main part (95.6%) of the emitted energy would be in the range [1.45; 14.5 μm]. This temperature level is often considered as relevant for vegetation fire (see for example comments on experimental measurements of fire temperatures in [6]) and the above-mentioned wavelength range is consequently well centered for the purpose of radiative property evaluation. It requires the use of devoted apparatuses in the infrared. In particular, a Fourier Transform InfraRed spectrometer and an infrared detector have been used in [9]. Note that common studies using IR camera in the frame of forest fire applications are often using devices whose wavelength window is not well suited for a fire study (often above 7.5 μm). Of course the information related to the emitted flux can be obtained but data must be taken with care as most of the non-grey phenomena occur below 7.5 μm and are not "viewed" by such a camera. This problem has been taken into account here with a camera allowing acquisitions between 2 and 14 μm. The sharp

\* Corresponding author. Tel.: +33 383 684 686.

E-mail address: [pascal.boulet@lemta.uhp-nancy.fr](mailto:pascal.boulet@lemta.uhp-nancy.fr) (P. Boulet).

## Nomenclature

$I$	Intensity, [ $\text{W m}^{-2} \text{sr}^{-1}/\text{cm}^{-1}$ ]
$T$	Temperature, [K]

### Greek symbols

$\epsilon$	Emissivity, [-]
$\nu$	wavenumber, [ $\text{cm}^{-1}$ ]
$\Phi$	Flux measured with spectrometer, [ $\text{W m}^{-2} \text{sr}^{-1}$ ]
$\varphi$	Flux measured with IR camera, [ $\text{W m}^{-2} \text{sr}^{-1}$ ]

### List of abbreviations

FTIR	Fourier Transform InfraRed
IR	InfraRed
RTE	Radiative Transfer Equation

spectral variations of the radiation emitted by flames raise an other difficulty. The range of interest is discussed above, through the emission of a high temperature surface, but the actual emission strongly varies with the wavelength. As a consequence, a quantitative evaluation of the emission must be undertaken with a spectral analysis. As we will see, an IR camera can still be used, but it must be coupled with filters that will allow the study of the spectral emission.

In the present study, the characterization of the emitted radiation has been addressed, using equivalent setups, aimed at the measurement of radiative fluxes emitted by flames, in the same wavelength range. Experimental data of emitted fluxes can be found in the literature, but generally total fluxes are concerned, with no or few indication on the wavelength distribution of the corresponding energy (see [6,7,10–12] for example). The study of the flame emission provides radiant emissive powers, total extinction coefficients or equivalent emissivities depending on the analysis which is carried out. Some attempts have been also devoted to the spectral characterization of fires on small burner flames in laboratory conditions. Bourayou et al. [13], then Ayranci et al. [14] for example presented a study of emission by flames using FTIR spectrometry. The role of various combustion products ( $\text{H}_2\text{O}$ ,  $\text{CO}_2$ ,  $\text{CO}$ , soots) has been observed. Study of the flame and information on the soot properties have been extracted from these observations, but it was in definite conditions in laboratory, for the flame of a specific gas burner. We applied a similar technique on vegetation fires in a previous study [15]. The aim was to study realistic vegetation flame. A second goal was to generate larger fires, still relatively small as compared to forest fires, but already in outdoor conditions. Observing fires of vine branches in trays, we registered the emitted radiation as a function of wavelength in the infrared. We noticed the strong contributions of the combustion gases, and the weak role of soots in this range. The corresponding work was considered as a preliminary step asking for a confirmation and for a better quantification of the emitted radiation. This second step has been addressed here combining an IR camera with the FTIR spectrometer and performing dedicated calibration tasks with a reference emitter. The problems of feasibility and repeatability had been already addressed in [15]. The setup presented here has taken benefit from this first experience and above all, from the two complementary observations in the infrared. In particular, new data on the soot contribution and on the quantitative emission have been obtained. One originality of the present work is the combination of the IR camera with 3 particular filters. This allows to isolate specific wavelength bands. The two devices (IR camera and FTIR spectrometer) are consequently observing the same flame, but they deliver complementary results obtained independently. The

second originality is an attempt to quantify the emission, whereas our previous paper [15] was mainly concerned with qualitative observations.

The paper reports on a collection of selected results and is organized as follows: the experimental setup is presented in a first section, then experimental results are presented and discussed including a description of the emission spectrum, an observation of the various contributors to the emitted radiation, and finally a comparison of the emission for two locations in the fire area.

## 2. Experimental setup

### 2.1. Device description

The experimental setup is presented in Fig. 1. The set of three images shows a general view of the setup, a zoom on the calibration device and a typical flame. The first basic element is an FTIR spectrometer (MATRIX by *Bruker*) combined with a dual detector InSb/HgCdTe (IR Associates), as already described in [15]. The main features of these apparatuses are merely recalled below. The spectrometer is classically built around a Michelson interferometer and a ZnSe window on the emission port, which is dedicated to the use of an external source, the fire itself in the present case. The dual detector system comprises two complementary IR detectors, an HgCdTe detector in the  $600\text{--}2000\text{ cm}^{-1}$  range and an InSb detector in the  $1900\text{--}6000\text{ cm}^{-1}$  range. The post-processing of measurements has been addressed in the range  $1000\text{--}6000\text{ cm}^{-1}$ . The common range  $1900\text{--}2000\text{ cm}^{-1}$  is useful for the manipulation of spectra by a merge process. The spectral resolution was taken to be  $4\text{ cm}^{-1}$ .

The second key element is an IR camera PV 320L by *Electro-physics*. This camera is built around a  $320 \times 240$  pyroelectric focal plane array. Its useful spectral range is well suited for the present application: between 2 and  $14\text{ }\mu\text{m}$  ( $700\text{--}5000\text{ cm}^{-1}$ ). The objective lens has a 35 mm focal length giving a  $25 \times 19^\circ$  field of view.

Selected filters can be added to the camera, with spectral transmission given on Fig. 2a. We have chosen these filters in order to focus on some specific contributions: around  $2247\text{ cm}^{-1}$  (or  $4.45\text{ }\mu\text{m}$ ) in order to observe the role of  $\text{CO}_2$ , around  $1277\text{ cm}^{-1}$  (or  $7.83\text{ }\mu\text{m}$ ) for the observation of  $\text{H}_2\text{O}$  contribution, and around  $2631\text{ cm}^{-1}$  (or  $3.80\text{ }\mu\text{m}$ ) where no hot gases are emitting, allowing to discriminate the role of soots.

The FTIR spectrometer and the IR camera are combined through the use of a beamsplitter that directs approximately half of the signal to each apparatus. This ensures that both apparatuses are observing simultaneously the same emitting surface. A preliminary calibration has been done with a black like surface indicating accurately the exact surface observed by the FTIR spectrometer in measurements conditions (in particular with a 3 mm aperture in diameter in order to limit the angle of view and the received flux). The IR camera is viewing a larger emitting surface but centered on the area viewed by the spectrometer. The spectrometer receives the flux in a solid angle virtually corresponding to a circular disk with diameter of 6 cm, located at 2 m from the entry window. This is approximately the distance between the flame and the IR devices, and this virtual circle will appear on the presented pictures reconstructed in false colors in the next section.

As a complement, photographs are also acquired in the visible range using a camera in order to keep a picture of the flame in the visible for further analysis and confirmation of the image reconstructed through IR acquisitions.

The fire is lighted in a square tray with size 50 cm and height 10 cm. Vine branches and *excelsior* are used for the fuel. A typical run uses this fuel in two layers: a first layer of approximately 5 cm of *excelsior* is put on the tray and vine branches are put in an upper

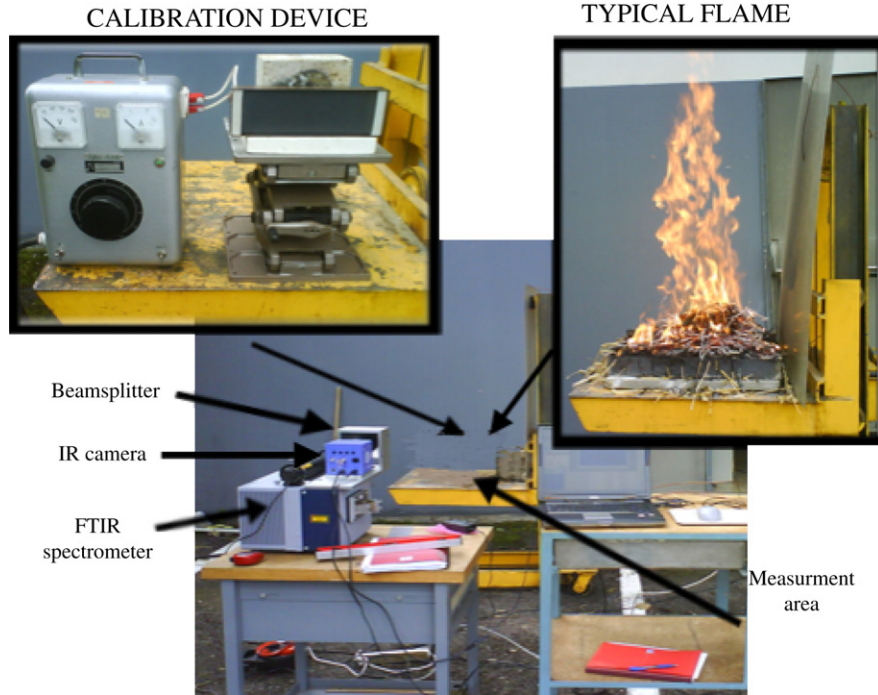


Fig. 1. Presentation of the experimental setup.

layer of approximately 10 cm. The respective loads are weighted in order to allow a better repeatability of the measurements. Typical loads are the followings: 200 g of *excelsior* plus 500 g of branches. No additional liquid fuel is required for the start of the fire as the flames are spontaneously developing on the residual embers of the preceding test, if needed with the help of a blower that is immediately stopped when the flame is ignited (note that the tray is emptied regularly and that these embers allow the ignition but correspond to a negligible load). This choice has been done in order to make sure that nothing else than the result of the pyrolysis of the vegetation does contribute to the production of the emission spectrum. A typical run lasts around 3 min with a fast ignition (around 30 s). All acquisitions are carried out after this ignition step, typically 1 min after the beginning of the run. The flame is fully developed, meaning that it has reached some stable regime conditions (no variation in time is studied at this stage and stationary conditions are sought). Since the flame is flickering, one cannot exactly speak of a stationary regime and the successive acquisitions can exhibit some variations, but as it will be seen the spectral variations and even the intensity levels are quite repeatable.

## 2.2. Data processing

Only a calibration with a well-known emitter can allow the production of a quantitative evaluation of the emitted fluxes. This has been done using blackbody-like emitters with a stabilized temperature and well-known emissivity (known as a function of the wavenumber and allowing an accurate correction of the emission). The basic idea is that the flux received by the spectrometer, or by the camera combined with one of the filters, from the reference emitter in definite temperature conditions, gives a reference value which is used in a second step to scale the values obtained by viewing the flame emission. This is a step of fine qualification of the device which has been conducted partly in the laboratory with a reference blackbody (M330EU by *Mikron*

*infrared*). In outdoor conditions some verifications must be also carried out between the different runs on the vegetation flame using a reference surface, but the blackbody cannot be used in these rough conditions. We consequently use a second reference emitter: a surface referred as *infraline* (by *Ittech System*) which behaves almost as a black surface (see on Fig. 1 the upper left picture of the outdoor calibration device). *Infraline* is an electrically-heated emitter with a surface of 15 cm by 6 cm (easy for the definition of the line of sight). Prior to its use, a calibration test of the *infraline* emission was also performed in our laboratory, by comparing the signal obtained in well-established conditions with that measured on the reference blackbody. "Well-established conditions" means that the *infraline* was at a distance of 2 m from the spectrometer, and was in thermal steady state when submitted to an electrical intensity of 5 A (as for outdoor experiments). One interesting feature in these conditions is that the corresponding emission is close to the one of a blackbody at 1000 K, the suitable emission range for a calibration.

In order to obtain quantitative information from the fluxes observed in arbitrary units, the exact following treatments are applied for the two IR devices of interest:

- For the IR camera data, the calibration is done observing the emission by the thermostated blackbody. This gives a correspondence between the camera signal ( $\varphi_{\text{ref}}$ ) and the temperature of the blackbody  $T_{\text{bb}}$ , and therefore a corresponding blackbody spectral intensity yielded with a Planck's law  $I_{\nu}(T_{\text{bb}})$ . Three calibration runs have been performed for each of the filters presented above. A background signal ( $\varphi_{\text{zero}}$ ) is measured prior to the calibration run. The result is a calibration curve fitting the data as  $I_{\nu} = f(\varphi_{\text{ref}} - \varphi_{\text{zero}})$ . Fig. 2b presents the corresponding calibration curves for the camera combined with each one of the three filters. Symbols are for the calibration runs and continuous lines have been obtained using a second order polynomial fit. When receiving the emitted flux from the flames in arbitrary

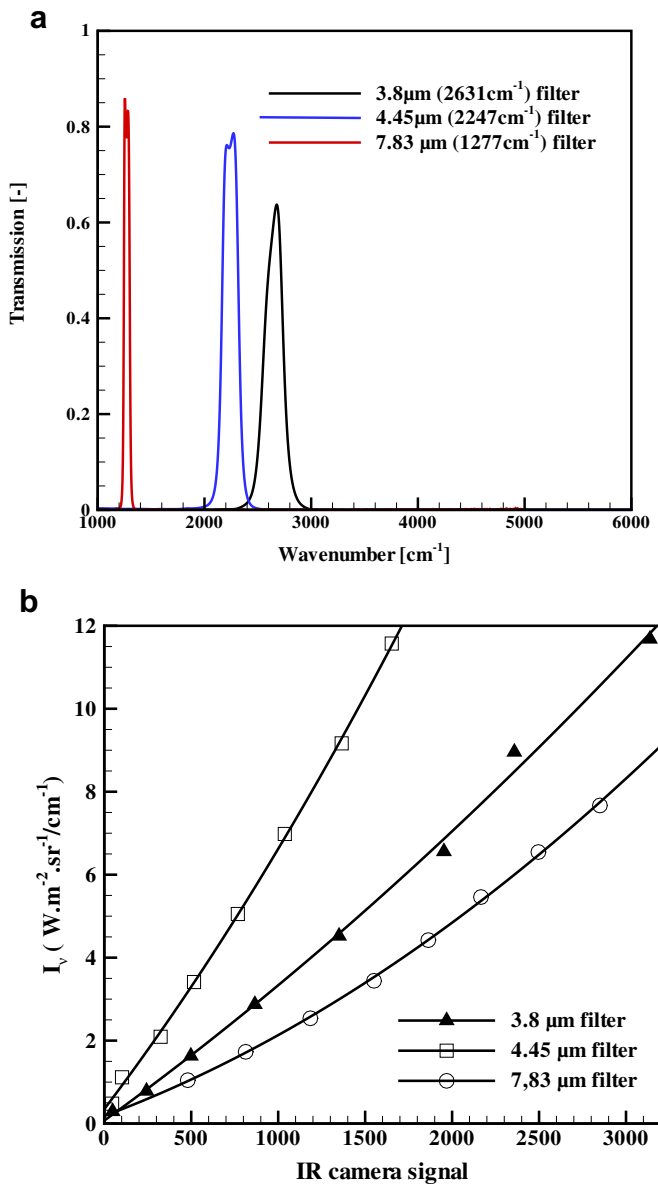


Fig. 2. Preliminary data regarding the IR camera qualification.

unit, a correspondence can now be done between the camera signal ( $\phi_{\text{flame}}$ ) and the emitted intensity  $I_\nu$ . A background correction has still to be done in order to extract the exact emission coming from the flame. We have chosen to use a threshold correction, identifying in an automatic processing the minimum signal registered by the camera in the IR picture in arbitrary unit (signal coming from outside of the flame area as the  $320 \times 240$  array receives the information from a field much larger than the flame only) and using it as the ( $\phi_{\text{zero}}$ ) value of the run. Then a direct use of the calibration data yield the intensity as  $I_\nu = f(\phi_{\text{flame}} - \phi_{\text{zero}})$  based on the polynomial fit.

(ii) For the FTIR spectrometer, the equivalent of a spectral intensity  $I_\nu$  is built comparing the flux received from the flame  $\Phi_{\text{flame}}$ , and from the reference emitter  $\Phi_{\text{ref}}$ . This comparison is done in identical outdoor conditions, but this reference emitter (*infraline*) has been previously calibrated with the thermostated blackbody at temperature  $T_{\text{bb}}$  in

laboratory conditions. Naming  $\Phi_{\text{bb}}$  the signal received from the reference blackbody, the post-processing is then a direct treatment as

$$I_\nu = \left( \frac{\Phi_{\text{flame}}}{\Phi_{\text{ref}}} \right) \left( \frac{\Phi_{\text{ref}}}{\Phi_{\text{bb}}} \right) I_\nu^* (T_{\text{bb}}) \quad (1)$$

### 3. Experimental results

A total of 74 runs have been performed, considering feasibility, repeatability tests, measurements with the various filters, acquisition in different areas of the flame. This section presents a selection of data regarding the information obtained with the IR camera, a combined analysis of the spectral data gained with both apparatuses, and finally some influence tests regarding the area of the flame viewed by the spectrometer.

#### 3.1. Infrared emission studied with the IR camera

Fig. 3 presents three runs carried out in the same conditions. Fig. 3(a) is a picture taken with a visible camera, whereas Fig. 3(b)–(d) are infrared pictures carried out at the respective wavelength bands around 7.83  $\mu\text{m}$ , 4.45  $\mu\text{m}$  and 3.80  $\mu\text{m}$ . All views have been taken at least 1 min after the ignition, in conditions of developed flame. The load is the same, the flame are very similar, with the typical shape that can be observed through the picture 3(a) (which has been taken at the same instant that Fig. 3d). However, the infrared pictures are very different because of the filters that isolate the contribution of gases and soots. Note the black circle on the views that corresponds to the area viewed by the spectrometer (discussed in the next paragraph). The following comments summarize our observations:

- Around 7.83  $\mu\text{m}$  (1277  $\text{cm}^{-1}$ ), the flame area is emitting but a stronger flux is coming from the bottom of the picture due to the burning vegetation area (maximum emitted intensity around  $6 \text{ W m}^{-2} \text{ sr}^{-1}/\text{cm}^{-1}$ ). The mean emission level from the flame itself is rather between 2 and  $3 \text{ W m}^{-2} \text{ sr}^{-1}/\text{cm}^{-1}$ . This wavelength band is characteristic of the emission by water vapor produced by the combustion. This constituent of the combustion gases is clearly seen to contribute in an obvious manner to the radiation emission.
- Around 4.45  $\mu\text{m}$  (2247  $\text{cm}^{-1}$ ), the infrared picture is different since much radiation is emitted by the flame area, even more than by the vegetation litter. The signal level is very high (maximum around  $12 \text{ W m}^{-2} \text{ sr}^{-1}/\text{cm}^{-1}$ ) and the contribution of  $\text{CO}_2$  (the investigated species in this range) is clearly seen to be of utmost importance.
- Around 3.8  $\mu\text{m}$  (2631  $\text{cm}^{-1}$ ), no gas is expected to contribute to the emission and the soots should be the only emission source in the flame area, but as can be seen the signal level is very low. What is still seen is the contribution of the litter, but the flame area is weakly emitting and the soots must be considered as a weak contributor to the overall emitted radiation (at least for the present small scale flame).
- Note, in all cases, the strong emission by the burning litter which emits radiation in the whole range of the infrared, whereas the flame itself only emits radiation in definite ranges of the infrared (it will be confirmed in the next section). It appears that the bottom part where the vegetation is burning has a larger emissive power than the flame itself and can play an important role in the global radiation emission. The flame should not be considered as the only contributor to the global

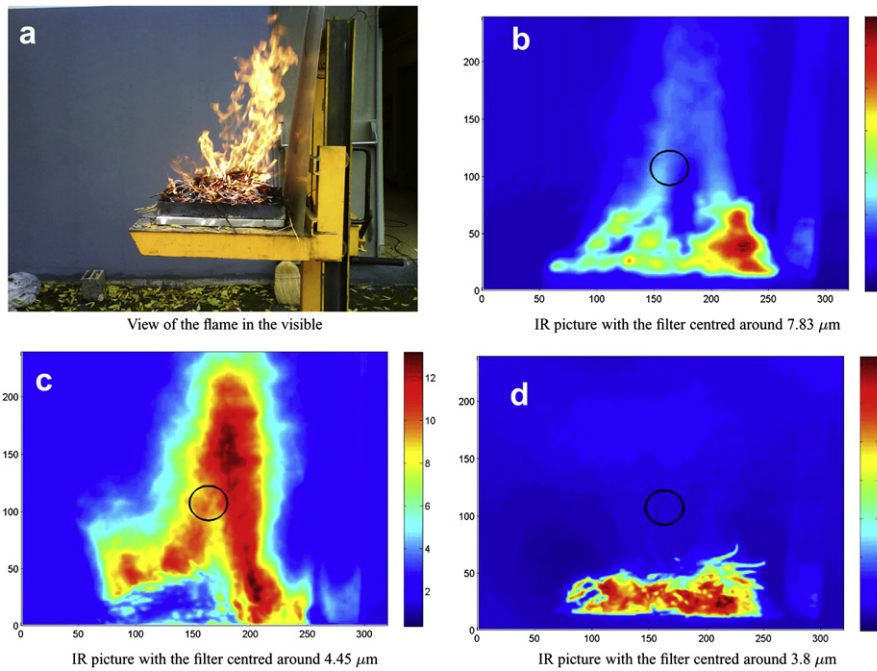


**Fig. 3.** Pictures of the flame in the visible range and in the infrared around 3.8, 4.45 and 7.83  $\mu\text{m}$ .

radiation emission, radiation is also coming from the basis of the fire.

### 3.2. Spectral analysis combining IR camera and FTIR spectrometer

A complementary spectral analysis is now done on the basis of the FTIR spectrometer results. Fig. 4 presents the spectra acquired at the same instant that the above-commented IR images of Fig. 3. The spectrometer angle of view is restricted to an area located in the flame approximately 10 cm above the burning litter. The corresponding area was indicated through the symbolic circles on Fig. 3. Since three different acquisitions are presented on this figure (this was not necessary for the spectrometer but for the IR camera

successively combined with one of the three filters), this gives an idea of the good repeatability of the measurement. As expected, the emission is far from being the one of a black or grey radiative panel at an hypothetical high temperature. The above comments are confirmed, with the high emission peak for  $\text{CO}_2$  around  $2300\text{ cm}^{-1}$ , some emission structures related to  $\text{H}_2\text{O}$  contribution in the ranges  $[1200\text{--}2000\text{ cm}^{-1}]$  and  $[3300\text{--}4200\text{ cm}^{-1}]$ , and finally the weak emission outside these gas contributions confirming the weak role of soots.

One interesting possibility is the comparison between the intensity levels given totally independently by the two apparatuses. On Fig. 4 the bandwidth of the three filters used with the IR camera are recalled through dotted lines. For each filter the limits of the bandwidth correspond to a transmission level equal to  $70.7\%$  of the maximum value ( $1/\sqrt{2}$ ). An average of the spectral emission in these bands has been done. In parallel on Fig. 3(b)–(d) the mean intensity has been computed inside the virtual circle viewed by the spectrometer (average of the pixels involved in each circle). Table 1 gives the corresponding results.

The agreement is better than simply qualitative, confirming the respective role of the flame constituents. Only in the case of Fig. 3b, related to the role of the vapor, the agreement is less satisfactory. We think that a better evaluation of the background emission with the IR camera should allow a finer evaluation. In any case, gases do contribute to the emission in a larger manner than soots, and both apparatuses are in accordance with this observation.

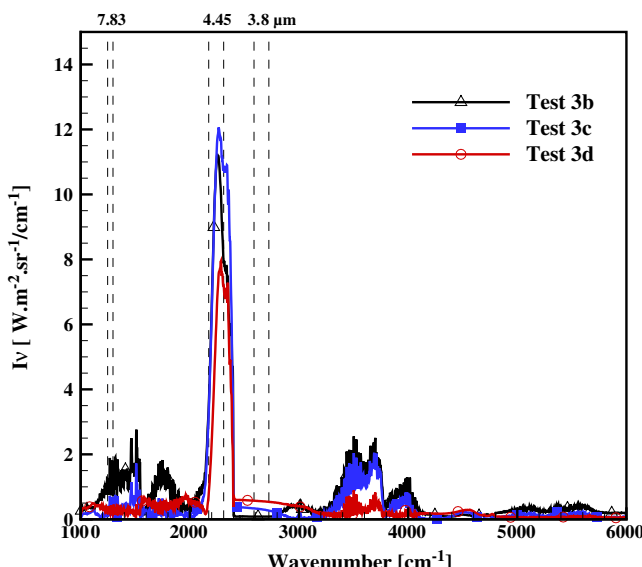


**Fig. 4.** Spectral intensity emitted in the flame 10 cm above the burning vegetation.

**Table 1**

Averaged intensities computed with both apparatuses, coming from the area indicated by the circles on Fig. 3(b)–(d) (in  $\text{W m}^{-2} \text{ sr}^{-1}/\text{cm}^{-1}$ ).

	Fig. 3(b) (around 7.83 $\mu\text{m}$ )	Fig. 3(c) (around 4.45 $\mu\text{m}$ )	Fig. 3(d) (around 3.80 $\mu\text{m}$ )
Average intensity for the spectrometer	1.8	9.6	0.6
Average intensity for the IR camera	1.2	9.3	0.6

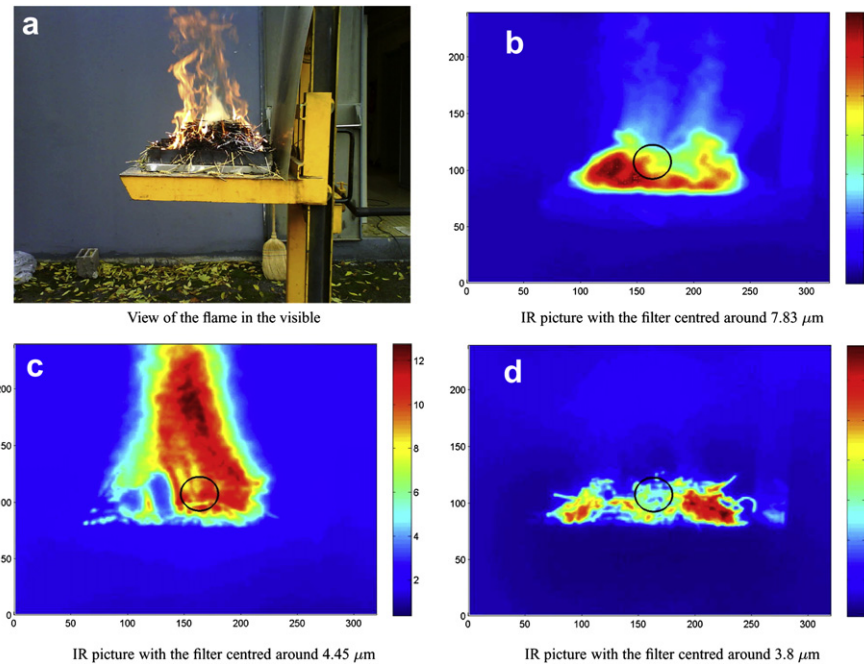


Fig. 5. Pictures of the flame in the visible range and in the infrared around 3.8, 4.45 and 7.83  $\mu\text{m}$ .

### 3.3. Comparison with the emission from the burning vegetation litter

An interesting comparison can be made with spectra acquired in the same conditions but with a line of sight coming from the burning vegetation in what concerns the spectrometer (see the new position of the circle on Fig. 5). For the IR camera, this does not change the acquisition conditions and the IR images given on Fig. 5(b)–(d) together with the visible image (5(a)) are presented in order to demonstrate the good repeatability of our acquisitions with the IR camera (when compared to Fig. 3(a)–(d)). As can be seen, the above given observations (Section 3.1) are still valid concerning the global view of the flame. What is different is the FTIR result, which is now characteristic of the burning vegetation. As presented on Fig. 6 the emission is clearly stronger and “visible” in the whole infrared range. Gas contributions are still observed, but superimposed with a high continuous emission. The actual curve has a global shape that qualitatively recalls the emission of a body at high temperature, but reduced assumption like black or even grey emission should be used with caution. This time we can also observe that for the three runs that have been conducted in the same conditions, the three spectra are in a qualitative agreement but the intensity levels are slightly different. The litter contribution seems to vary quantitatively from run to run (and probably during the run itself), even if the global shape of the spectral curve is the same. This burning area is confirmed to be a very important radiation emitter and could be considered like a radiant panel, whereas the flame probably exhibits a larger emission surface but with a less effective emission capability in terms of heat flux density. Like in the previous section a quantitative evaluation has been done based on the radiation received by each apparatus independently (Table 2). The global agreement between the two acquisition techniques is confirmed, in this case of a higher emission level as above explained.

In order to provide an estimation of the total radiative energy produced by the flame, an integration of the emission spectra over the wavelength band of measurement has been also done. The

cases corresponding to the flames referred on Figs. 3(b) and 5(d) have been addressed. This yields the following results: the corresponding flame itself emits  $4.3 \text{ kW m}^{-2} \text{ sr}^{-1}$ , whereas the litter presented through Fig. 5(d) emits  $12.8 \text{ kW m}^{-2} \text{ sr}^{-1}$ . For a comparison, a blackbody at 1000 K in the same wavelength range would emit  $16.0 \text{ kW m}^{-2} \text{ sr}^{-1}$ . Consequently, one possible rough description of the burning litter area would be a radiant panel with temperature 1000 K and total emissivity 0.8. This would at least provide the right radiant emissive power. For the flame, the same rough analysis would yield an emissivity of 0.27 for the same temperature. However, we do not recommend such description for the flame that makes use of an equivalent temperature which is

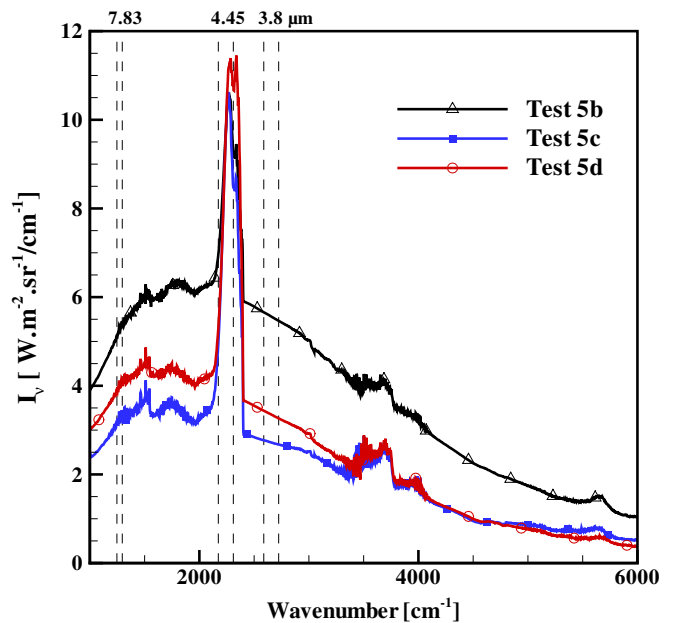


Fig. 6. Spectral intensity emitted by the burning vegetation area.

**Table 2**

Averaged intensities computed with both apparatuses, coming from the area indicated by the circles on Fig. 5(b)–(d) (in  $\text{W m}^{-2} \text{sr}^{-1}/\text{cm}^{-1}$ ).

	Fig. 5(b) (around 7.83 $\mu\text{m}$ )	Fig. 5(c) (around 4.45 $\mu\text{m}$ )	Fig. 5(d) (around 3.80 $\mu\text{m}$ )
Average intensity for the spectrometer	4.4	9.6	2.6
Average intensity for the IR camera	5.3	8.6	3.3

questionable for such a complex medium, and a total emissivity that hides the complex non-grey behavior of the flame revealed by the various spectra. In particular the suggestion of a temperature around 1200 K and an emissivity equal to 0.13 would also produce the same radiative flux and there is no way with the present data to justify the use of one set of parameters or the other. The discrepancy between the equivalent emissivities 0.2 and 0.8 also confirms the respective roles of the flame and the litter area in the radiation emission. However such data should be used with care because the spectral emission itself has been observed to be different, depending on whether the flame or the litter is seen. Another important point is that the present flames are still relatively small. We expect that larger flames would be more loaded in soots and would consequently emit radiation in a stronger manner.

#### 3.4. Radiation emission versus vegetation absorption

Considering some of our recent results regarding the absorption of the vegetation [9,16], a final comparison is done between the spectral emission which has been measured here and the absorption of one characteristic vegetation species involved in forest fires: pine needles. The data of dry needles in thick layer are used here (like fallen needles on the floor). Two characteristic emission spectra have been selected and normalized using their maximum values in order to allow the comparison of the spectral evolutions. It is seen that the vegetation absorption is maximum below 4000  $\text{cm}^{-1}$  (up to 0.97) where the flame emission is the highest, a particularity that will unfortunately favor the radiation absorption, and consequently the fire propagation through radiation (Fig. 7).

An averaged absorptivity  $\langle \alpha \rangle$  can be computed using the spectral emission  $I_\nu$  given here as the incident radiation, in the following manner:

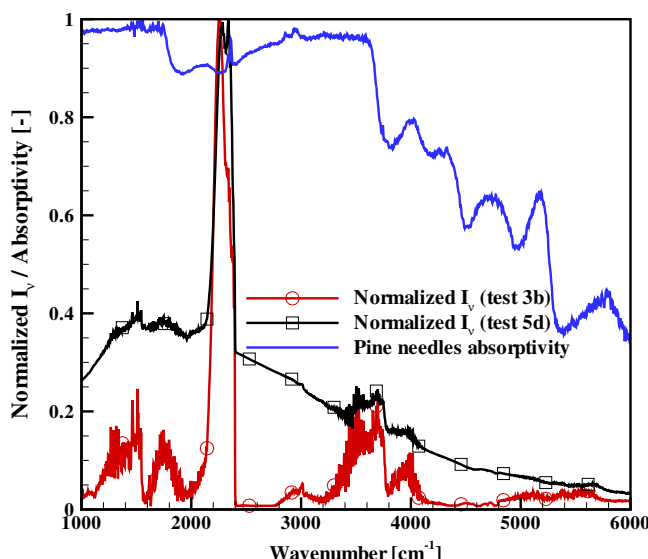


Fig. 7. Normalized spectral emission compared to absorption of a litter of pine needles as a function of wavelength.

$$\langle \alpha \rangle = \frac{\int \alpha_\nu I_\nu d\nu}{\int I_\nu d\nu} \quad (2)$$

The following values are obtained: 0.87 when considering the flame as the radiation source and 0.89 with the litter emission, which provides very close results and gives an idea of the discrepancy between the characteristics of a true vegetation and the classical assumption of a black surface.

#### 4. Conclusions

A series of measurements has been carried out combining the observation in the infrared with an FTIR spectrometer and an IR camera, taking a picture at the same time in the visible with a camera. Both IR apparatuses confirm the large contribution of emission around 2300  $\text{cm}^{-1}$  by  $\text{CO}_2$ , the important emission by  $\text{H}_2\text{O}$ , and the weak contribution of soots. The emission is consequently far from the one of a black surface or even a grey surface at high temperature. The area of burning vegetation emits in a stronger manner and in a continuous way in the infrared.

If the present work is considered for a possible application in simple models assuming that the flame is a kind of radiant panel, the analysis shows that the total radiant power from the flame is equivalent to the one of a grey medium with temperature 1000 K and emissivity just below 0.3. However, radiation should be also taken into account as coming from the bottom part of the flame, corresponding to the surface of the burning vegetation itself, emitting radiation like a surface at 1000 K with an emissivity equal to 0.8. Considering the obvious non-grey behavior of the flame, a finer description, but demanding a higher computational effort, has to involve a band model taking into account a major contribution for  $\text{CO}$  and  $\text{CO}_2$  gases around 2300  $\text{cm}^{-1}$ , and  $\text{H}_2\text{O}$  bands in the ranges [1200–2000  $\text{cm}^{-1}$ ] and [3300–4200  $\text{cm}^{-1}$ ]. A continuous contribution over the whole spectrum could be also considered for the bottom area of the flame and may be for the soot radiation but the determination of the corresponding radiant power will require supplementary investigations.

On the basis of the present outdoors experiments, complementary information could be now obtained considering large scale fires in order to see if the soot contribution rises with the optical thickness of the flame. Time evolution and spatial variations are two other topics that could receive supplementary investigations at realistic scale flames.

#### Acknowledgements

This research is supported by the French National Research Agency (ANR) – “PIF” project (Protection contre les Incendies de Forêts) through contract 0264-01.

#### References

- [1] D.X. Viegas, Forest fire propagation. *Philos. Trans. R. Soc. Lond. A* 356 (1998) 2907–2928.
- [2] J.F. Sacadura, Radiative heat transfer in fire science. *J. Quant. Spectrosc. Radiat. Transf.* 93 (1–3) (2005) 5–24.
- [3] R. Viskanta, Overview of some radiative transfer issues in simulation of unwanted fires. *Int. J. Therm. Sci.* 47 (2008) 1563–1570.
- [4] B. Porterie, J.L. Consalvi, J.C. Loraud, F. Giroud, C. Picard, Dynamics of wildland fires and their impact on structures, 149 (2007) 314–328.
- [5] D. Morvan, S. Méradj, G. Accary, Physical modelling of fire spread in grasslands. *Fire Saf. J.* 44 (2009) 50–61.

- [6] P.A. Santoni, A. Simeoni, J.L. Rossi, F. Bosseur, F. Morandini, X. Silvani, D. Cancellieri, J.H. Balbi, L. Rossi, Instrumentation of wildland fire: characterisation of a fire spreading through a Mediterranean shrub. *Fire Saf. J.* 41 (2006) 171–184.
- [7] G.C. Vaz, J.C.S. André, D.X. Viegas, Estimation of the radiation extinction coefficient of natural fuel beds. *Int. J. Wildland Fire* 13 (1) (2004) 65–71.
- [8] K. Chetehouna, O. Séro-Guillaume, A. Degiovanni, Measurement of radiative absorption coefficient for a vegetal medium. *Meas. Sci. Technol.* 15 (6) (2004) N43–N46.
- [9] B. Monod, A. Collin, G. Parent, P. Boulet, Infrared radiative properties of vegetation involved in forest fires. *Fire Saf. J.* 44 (1) (2009) 88–95.
- [10] J.L. Dupuy, P. Vachet, J. Marechal, J. Melendez, A.J. de Castro, Thermal infrared emission-transmission measurements in flames from a cylindrical forest fuel burner. *Int. J. Wildland Fire* 16 (2007) 324–340.
- [11] B.W. Butler, J. Cohen, D.J. Latham, R.D. Schuette, P. Sopko, K.S. Shannon, D. Jimenez, L.S. Bradshaw, Measurements of radiant emissive power and temperatures in crown fires. *Can. J. For. Res.* 34 (2004) 1577–1587.
- [12] E. Pastor, A. Rigueiro, L. Zarate, A. Gimenez, J. Arnaldos, E. Planas, Experimental methodology for characterizing flame emissivity of small scale forest fires using infrared thermography techniques. in: D.X. Viegas (Ed.), *Proceedings of the 4th Int. Conf. on Forest Fire Research, Luso-Coimbra, Portugal*. Millpress, Rotterdam, Netherlands, 2002 CD-Rom.
- [13] I. Bourayou, R. Vaillon, J.F. Sacadura, FTIR low resolution emission spectrometry of a laboratory-scale diffusion flame: experimental set-up. *J. Quant. Spectrosc. Radiat. Transf.* 26 (2–4) (2002) 181–187.
- [14] I. Ayrancı, R. Vaillon, N. Selçuk, Near-infrared emission spectrometry measurements for nonintrusive soot diagnostics in flames. *J. Quant. Spectrosc. Radiat. Transf.* 109 (2) (2008) 349–361.
- [15] P. Boulet, G. Parent, A. Collin, Z. Acem, B. Porterie, J.P. Clerc, J.L. Consalvi, A. Kaiss, Spectral emission of flames from laboratory-scale vegetation fires, *Int. J. Wildland Fire*, in press.
- [16] Z. Acem, G. Parent, B. Monod, G. Jeandel, P. Boulet, Experimental study in the infrared on the radiative properties of pine needles. *Fire Saf. J.*, Submitted for publication.